X-Ray mapping and the mineralogy pattern of nickel laterite ore: Bavanat, Fars, Iran

A. Abbasi Gharaei[1], B. Rezai[2*] and H. Hamidian Shoormasti[3]

1. Department of Mining Engineering, Science and Research Branch, Islamic Azad University, Tehran, Iran
2. Department of Mining and Metallurgy Engineering, Amirkabir University of technology (Tehran Polytechnic), Tehran, Iran
3. Department of Mining Engineering, Qaem Shahr Branch Islamic Azad University, Qaem Shahr, Iran

Keywords	Abstract
Laterites *Nickel* *Mineralogy* *EDS Line Profile Analyses*	According to the classification of the nickel laterite, this paper describes mineralogy test is to reveal where valuable elements are located in the ore, in which mineralogical form. The purpose of the sieving test was to study if some specific particle size contains most of the valuable metals. Based on its chemical composition nickel laterite is classified as a limonite type and the nickel and cobalt content was 0.7 and 0.04%, respectively. Nickel is predominantly associated with hematite and goethite. Based on the mineralogical analysis of the ore, it is observed that remarkable part of nickel is located in hematite. Therefore, nickel cannot be released from hematite lattice. The nickel content in the laterite was 0.7% and the cobalt content 0.04%. The chemical composition of laterite equals with the occurrence of 38.9% iron oxides, 26.9% carbonates, 26.9% quartz, 4.8% chromite, 2.7% magnetite and 1.9% other minerals. EDS line profile analyses were completed on hematite/goethite ooids and there was a slight correlation in the quantities between iron and nickel in each individual ooid. However, iron and nickel do not always show a positive correlation. Nickel grade could be enriched from 0.7 wt.-percent to 0.91 wt.-percent; however nickel recovery was only 45%.

1. Introduction

Conventionally, acid leaching methods are employed for the extraction of Ni from low-grade Ni laterite ores [1]. Despite the advances made to date, significant challenges associated with metallurgical and geotechnical extraction processes persisted. For relatively higher grade ores (~2 wt.% Ni), high-pressure acid leaching (HPAL), which is fast and aggressive but expensive method can be employed [2-4]. For a lower grade, more cost-effective processes of the heap leaching (HL) and atmospheric leaching (AL) are preferred [5]. Whilst HL is more economically competitive in terms of both capital and operating expenditures (CAPEX and OPEX) than AL, it is a very slow (100-300 days) process which for Ni laterites is faced with intractable geotechnical, hydrological and metallurgical

challenges [6, 7]. Consequently, to date, there exists only one plant in the world that conducts a commercial Ni laterite HL operation, the Minara Murrin plant in Australia [8, 9]. The relatively faster (e.g., 4-10 h) AL, operates in agitated tanks at elevated temperatures (e.g., 70-95 $^{\circ}$C) is a preferred route if certain optimum conditions can be maintained for high extraction rates (e.g., 80-90%) at acceptable lixiviant consumptions [10-12]. Hydrometallurgical processes including Caron process, HPAL, HL, and AL are widely used for processing low-grade (<1.1-2.0%) Ni laterites [2], [13-15]. The AL process, which is commonly used for the extraction of value metals (e.g., copper, gold) from their low-grade ores at lower capital and operating costs compared with HPAL [16-18]. AL

process involves contacting finely ground ore slurry with concentrated acid (e.g., H_2SO_4) to leach metal species into the aqueous phase. The process which is non-selective is carried out below water boiling point (<100 $^{\circ}$C) at atmospheric pressure in agitated vessels.

For low-grade ores (e.g., < 2 wt.% values), less energy intensive AL, generally performs at temperatures 70-95 $^{\circ}$C in agitated vessels is commonly employed [12,19]. Gangue mineralogy-mediated pulp chemistry changes which occurred during leaching sometimes lead to certain rheological behavior which was detrimental to value metal recovery [19-22]. The interactions between the mineral particles across the aqueous phase containing protons and dissolved species determines the particle interactions which directly define slurry's flow and deformation behavior in response to shear provided by agitation [23]. The solution viscosity is inversely related to the diffusivity of the reacting and product species in the aqueous phase and where it is markedly high, volume diffusion or mass transfer limitation becomes important. Intractable pulp rheology not only would lead to poor value metal recovery but also difficulty in pulp transport or pumpability and poor solid-liquid separation [12, 24-26]. For improved processability, therefore, appropriate assessment and due understanding of both leaching and rheological behavior, and their links, of the various mineral components (e.g., hematite and quartz) which predominated low-grade lateritic ores are warranted.

Complex, low-grade lateritic ores containing valuable metals (e.g., Ni, U) characteristically contain large quantities of clays (e.g., kaolinite and smectite) and oxides (e.g., goethite and hematite) as host gangue minerals [19, 27]. The value metals are often finely disseminated in the gangue minerals which tend to be poorly liberated [28]. This means that physical separation to upgrade the ore for smelting or HPAL is not technologically feasible [29]. Consequently, more cost-effective processes such as AL were employed in agitated tanks. Alumino-silicate clay and oxide gangue mineral phases in complex ores sometimes leads to challenges such as high acid consumption and processing difficulties (e.g., mixing, pumping, solid-liquid separation) during AL [9,22,30,31]. The gangue minerals-mediated pulp chemistry changes and particle interactions during leaching are believed to play pivotal roles in pulp behavior.

From the literature, the overall $H2SO4$ atmospheric leaching behavior of Ni laterite ores strongly is dependent on ore mineralogy and chemical composition and process conditions [26, 32, 33]. As lateritic ores with a similar composition could still display substantially different leaching behavior [12], AL process cannot be easily adapted to all ore bodies without appropriate background studies.

HPAL is best suited for the treatment of limonitic ores, although the Al and Mg contents should not be too high as they lead to an increased acid consumption [34]. It is generally regarded as the main commercial alternative to the Carbon process. The leached slurry is then transferred to flash cooling, neutralization, liquid/solid separation (via Counter Current Decantation (CCD)), solution purification and Ni and Co recovery [13, 14, 35, 36]. The use of expensive titanium autoclaves, high leach temperatures, and narrow leachable ore types usually put economic constraints on using HPAL for processing low-grade Ni laterites [36].

Ideally, leaching at higher solid loading is preferred as it would lead to increased throughput for the minerals' industry. However, as other operational factors (e.g., the concentration of free acid) could be limiting, the selection of the appropriate solid loading with leaching is vital in enhancing the overall process efficiency. Reported studies of the leaching of Ni and Co has shown that variation in pulp density could have a significant impact on leaching kinetics [29, 37-42]. It is reported by [38] that the percent of Ni and Co extractions during high-pressure $H2SO4$ leaching of maghemite/magnetite Ni laterite ore increases to a maximum as the acid to ore mass ratio increased from~0.20 to 0.55.

This paper described mineralogy and the classification of the nickel laterite in Fars province, Iran (probable deposit reserves $\approx$ 4 Mt). In addition, leaching tests are carried out to confirm that nickel laterite is amenable to nickel leaching. Two AL tests and two HPAL tests with laterite were carry out. Specifically, this work focuses on the links between pulp mineralogy and chemistry, particle interactions, process conditions and acid leaching behavior of lateritic minerals.

2. Materials and methodology
2.1. Ore sample pre-treatment
2.1.1. Crushing and grinding of ore samples
Laterite ore sample (80 kg) was crushed into 100% -1mm and for leaching tests were ground in a ball mill to 80% of -56 μm fineness. Grinding

time was 20 min and one grinding batch included 3.5 kg laterite, 22 kg balls and 3.5 kg of water for 50% slurry density.

2.1.2. Mineralogical characterization of nickel laterite ore

Purpose of the mineralogical test was to reveal where valuable elements were located in the ore, and in which mineralogical form. The purpose of the sieving test was to study if some specific particle size contains most of the valuable metals. The bulk sample material was used as the basis of the mineralogical study. The contents of the bulk material were sieved into size fractions using 2360 µm, 1180 µm, 850 µm, 600 µm, 425 µm, 300 µm, 212 µm, 150 µm, 106 µm, 75 µm, and 45 µm sieves to determine the grain size distribution. This resulted in a P_{80} of 910 µm. The particle size distribution was shown in Figure 1 (or Table 1). Before completing mineralogical studies, X-Ray diffraction (XRD) was used to identify the main mineral phases. Polished resin sections were prepared from the bulk sample and the mineralogy was studied by optical microscopy using a Zeiss Axioplan2 reflected light microscope equipped with an AxioCam ECs 5s camera. Polished samples were then carbon coated for mineralogical study using the JEOL 6940LV scanning electron microscope (SEM) equipped with an Oxford Instruments energy dispersive spectrometer (EDS). The chemical composition of the bulk sample was analyzed by ICP-OES (inductively coupled plasma optical emission spectrometry) after total dissolution and ICP-MS (inductively coupled plasma mass spectrometry). Fire assay was used to calculate the amount of gold and silver in the sample. An Eltra CS-2000 automatic analyzer was used to analyze the carbon and sulfur contents and SiO_2 was analyzed colorimetrically. The overall elements analyzed were As, Au, Ag, Ca, Cd, Co, Cr, Cu, $Fe_{tot,}$ K, Mg, Mn, Na, Ni, P, Pb, Sb, Sc, Se, Ti, and Zn. The mineral composition of the studied materials was based on information and observations from: XRD, optical microscopy, scanning electron microscopy with EDS of identified minerals, and the analyzed chemical composition of the sample. Mineral quantification was performed using HSC-Chemistry ®.

Table 1. Grain size distribution of the bulk sample material.

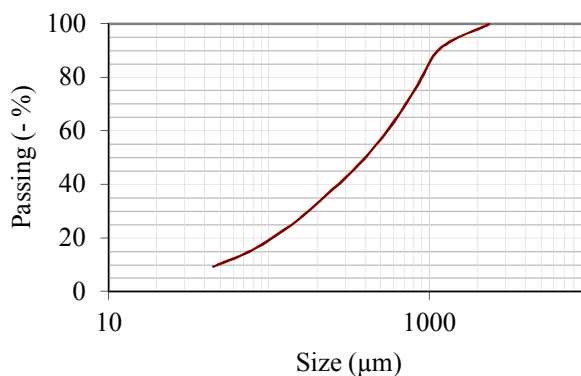| Sieve (µm)	Retained		Passing (%)
	g	%	
2360	0.3	0.2	99.80
1180	13	8.83	90.97
850	20.1	13.65	77.33
600	20.7	14.05	63.27
425	16.7	11.34	51.93
300	13.8	9.37	42.57
212	12	8.15	34.42
150	11.6	7.88	26.54
106	9.2	6.25	20.30
75	8	5.43	14.87
45	8.1	5.50	9.37
-45	13.8	9.37	0.00
Total	147.3	100	

Figure 1. Grain size distribution of the bulk sample material. P_{80} = 910 µm.

2.2. Mineralogy

The mineralogy of the nickel laterite material was studied by using optical microscopy methods as well as the Scanning Electron Microscope (SEM). The primary mineral grains were found as ooids or as spherical particles (Figure 2) consisting principally of hematite (Fe_2O_3), goethite (FeO[OH]) and minor amounts of locked chromite containing aluminum and magnesium ($FeCr_2O_4$).

The ooids typically showed concentric layers of varying compositions but were mostly found as hematite with inner or outer layers of goethite. Small amounts of anhedral magnetite were intermittently encountered within these ooids as well. The ooids were porous and were often filled with fine grains of quartz. Most of the grains had some fractures radiating from the nucleus. Nickel was carried predominantly by hematite and goethite but was rarely sometimes found within magnetite. Hematite and goethite also contained minor amounts of aluminum (1.79 wt. %), silica (3.84 wt. %), and chromium (1.35 wt. %). The average and median compositions were shown in Table 2. The amount of nickel within hematite was slightly more than goethite on average. Hematite contained an average of 1.89 wt% Ni, while goethite contained an average of 1.43 wt%. A majority of the analyzed magnetites contained no nickel, however, a few grains contained up to 0.95 wt% Ni. The composition of iron oxides and hydroxides should be considered an approximation as a result of the EDS analyses being unable to differentiate among the different valence states of iron, as well as it being unable to detect the amount of hydroxyl (OH$^-$) present within goethite.

Chromite was commonly encountered and on average contained high contents of Mg (5.49 wt. %) and Al (9.98 wt. %). It was appeared within sedimentary particles, within the ooids, or as euhedral grains. No chromite was found to contain any nickel. Other common minerals within the sample were quartz and various carbonates that appear within large sedimentary particles. Carbonates were primarily dolomite ($CaMg[CO_3]_2$), and calcite ($CaCO_3$), with appearing of some lesser amounts of Ankerite $Ca(Fe,Mg,Mn)(CO3)2$. Magnetite and small amounts of Subhedral Hematite were occasionally encountered within the sedimentary particles. Small quantities of euhedral iron-bearing sulfide minerals were observed, such as Arsenopyrite, Pyrite, and Pyrrhotite ($Fe_{(1-x)}S$ (x = 0 to 0.2)). Extremely fine grains (<10 µm) of variable composition copper oxides were found within grain fractions and porous areas of the iron oxide ooids. In addition, very small amounts of native platinum iridium, and gold were found as fine grains in the pores of the ooids with grain sizes appearing under 5 µm. One grain of Asbolane, a nickel-bearing clay mineral, was observed, however no subsequent grains were found. It is also the only clay mineral that was found within the sample that contains significant nickel. Other minerals that were found in sporadic amounts were altered Relict Olivine and Pyroxene minerals which contain minor amounts of nickel. As a result of the observed minerals within the bulk material, the nickel laterite in this study could be classified as a Limonite-type ore. This was due to the large quantity of iron oxide and iron oxide-hydroxide minerals present, and the significant scarcity of serpentine and clay minerals. Sieving of the laterite did not show to bring any significant benefit to recovery of nickel.
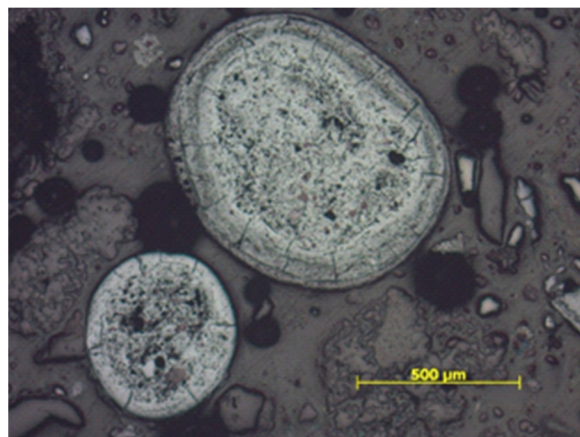

Figure 2. Typical appearances of hematite and goethite ooids rising within the nickel laterite sample. These were the typical mineral appearances and contained most of the nickel within the sample.

Table 2. Average and median chemical compositions measured by EDS of hematite and goethite grains within the nickel laterite sample.

Avg.	n.	O%	Mg%	Al%	Si%	Ca%	Cr%	Fe%	Ni%	Cu%
Hematite	199	26.81	0.38	1.48	3.68	0.23	1.32	63.86	**1.89**	0.21
Goethite	69	33.77	0.62	2.67	4.24	0.11	1.43	55.42	**1.43**	0.05
Combined	268	28.55	0.44	1.79	3.84	0.20	1.35	61.72	**1.78**	0.17
Median	n.	O%	Mg%	Al%	Si%	Ca%	Cr%	Fe%	Ni%	Cu%
Hematite	199	27.17	0.74	1.31	2.74	0.22	1.05	64.58	**1.53**	0.88
Goethite	69	33.8	0.7	2.81	3.95	0.16	1.38	55.79	**1.36**	0.81
Combined	268	27.92	0.71	1.63	3.14	0.23	1.11	61.84	**1.46**	0.84

2.3. Volume and ratio of hematite and goethite

Although it was not possible to calculate the amount of goethite and Hematite within the laterite sample separately, some calculations could be made based on the volume of grain size measurements. Ten different ooids were measured to determine the ratio of hematite and goethite present within an ooids. Most grains feature a hematite nucleus with a goethite shell. In a cross-section image tends to make the amount hematite appear much larger than goethite (Figure 3). However, as these images were not a three-dimensional representation, simple measurements were made to determine the approximate spherical volume of each of the ooids.

The inner diameter measurement was representative of hematite, whereas the outer was representative of the whole ooids. Using these measurements for spherical volume calculations, the volume of goethite and hematite could be approximated. The difference between the two volume measurements gave the volume of the outer goethite shell. Results of the ten measurements could be viewed from Table 3.
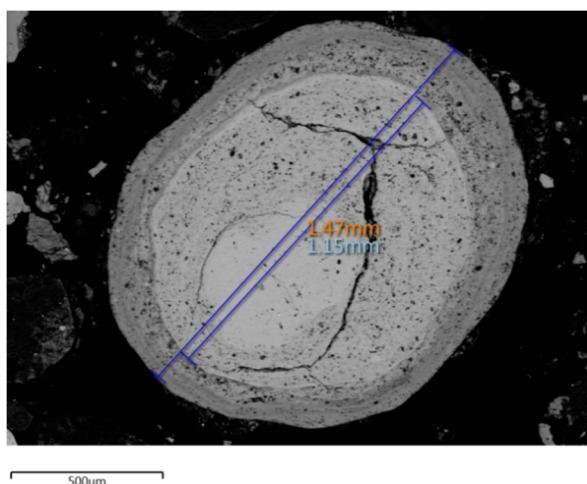
Figure 3. Cross-section image of iron oxide ooids.

Table 3. Calculated volumes of iron oxide ooids.

n.	Inner Diam. (mm)	Outer Diam. (mm)	Ooid Volume (mm^3)	Hem. Vol. (mm^3)	Goethite Vol. (mm^3)
1	1.15	1.47	1.66	0.80	0.87
2	1.22	1.38	1.38	0.95	0.43
3	0.555	0.842	0.31	0.09	0.22
4	0.81	0.841	0.31	0.28	0.03
5	1.35	1.56	1.99	1.29	0.70
6	1.34	1.5	1.77	1.26	0.51
7	0.571	0.781	0.25	0.10	0.15
8	0.83	0.965	0.47	0.30	0.17
9	0.315	0.5	0.07	0.02	0.05
10	0.64	0.89	0.37	0.14	0.23

2.4. Chemical and mineralogical composition

Based on the chemical assays made by ICP-OES, the bulk sample contained 27.4 wt. % SiO_2, 23.6 wt. % Fe, and Ca 5.59 wt. % as the major constituents. Other components of the bulk sample could be seen in Table 3. In order to quantify the minerals present within the bulk sample, hematite and goethite were combined into one group titled 'Fe-Oxides'. Similarly, this was done with carbonate minerals as well. Hematite and goethite were the main minerals and make up 38.87% of the sample. Carbonates (26.92%) and quartz (26.88%) were the most common gangue minerals and together total over 50% of the minerals found within the laterite (Table 4). Chromite and magnetite constituted 4.77% and 2.7% of the laterite, respectively. Other minerals (1.87%) consisted of other gangue minerals and the only nickel-bearing minerals being minor amounts of altered olivine and pyroxenes.

A typical ooids containing hematite, goethite, and a large grain of Mg-Al chromite was X-ray mapped using EDS and illustrates the distribution of nickel. As chromite did not contain any nickel,

there was a sharp contact visible between the chromite and goethite/hematite as was shown in Figure 4.

Nickel distribution was confined predominantly to hematite and goethite (93.23%). A minor amount of nickel was present within chromite and magnetite. Other minerals carried a total of 5.14% nickel, and they included the relict pyroxenes and olivine that is only found in trace quantities. The distribution of main elements could be found from Table 5. Magnesium was carried mostly within dolomite and some within chromite. Iron oxides often carried a small percentage of magnesium as well. Iron was mostly distributed within hematite, magnetite, and goethite as expected. However, small amounts were present in chromite and the carbonate minerals. Aluminum was mostly carried within goethite, hematite, and chromite and was present in minor amounts within magnetite and carbonates. Silicon was mostly found in quartz, though some was found within hematite and goethite. Chromium was mostly found within chromite, but some was also found within the hematite and goethite grains.

Table 4. Chemical and mineralogical composition of the bulk nickel laterite sample.

Element	Method	Unit	Bulk Sample	Mineralogy	Wt. %
Mg	TOT	%	3.74	Fe-Oxides	38.87
Al	TOT	%	1.44	Carbonates	26.92
K	TOT	%	0.1	Quartz	26.88
Ca	TOT	%	5.59	Chromite	4.77
Ti	TOT	%	0.05	Magnetite	2.7
Cr	TOT	%	2.17	Others	1.87
Mn	TOT	%	0.19	Total	100
Fe	TOT	%	23.6		
Co	TOT	%	0.04		
Ni	TOT	%	0.7		
Cu	TOT	%	0.01		
Zn	TOT	%	0.02		
C	Eltra	%	3.09		
SiO_2	Col.	%	27.4		
Sc	ICP-MS	ppm	37		
Au	FA	ppm	0.03		
Ag	FA	ppm	1.6		
Satmagan		%	2.7		

2.5. EDS line profile analyses

The purpose of the EDS analysis was to study if nickel concentration was related to any other element concentration (for example Fe) in the laterite. Approximately 300 data points were used to find any indication that nickel concentration is either elevated or depressed in the presence of other elements. Elements compared were: Al, Mg, Fe, Cr, O, and Si. The results were that nickel

element concentration shows no true correlation between its appearance and any other element. EDS line profile analyses were completed on hematite/goethite ooids and there was a slight correlation in the quantities between iron and nickel in each individual ooids. However, iron and nickel did not always show a positive correlation. In some grains, there was a negative correlation between nickel and iron (Figures 5 and 6).
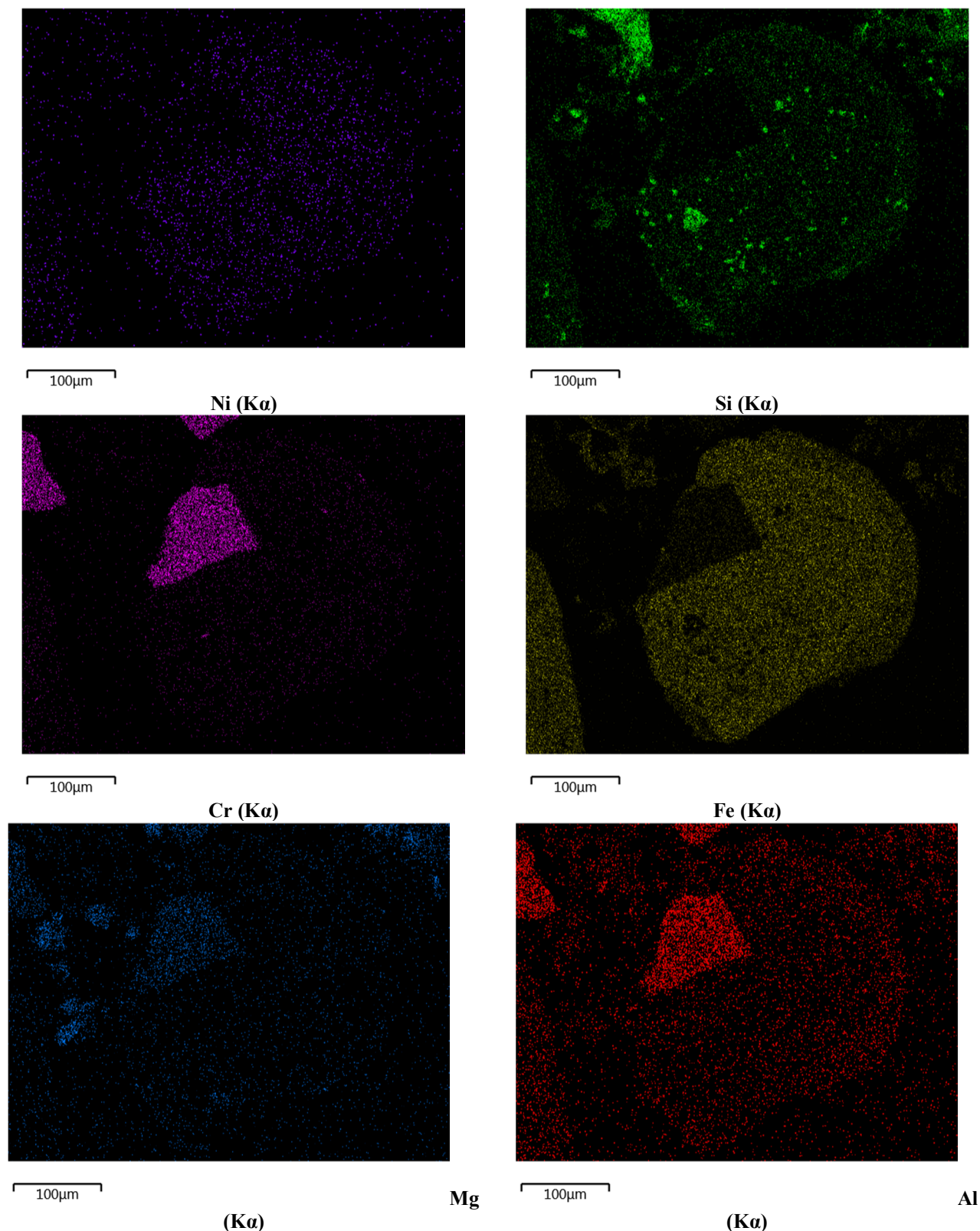
Figure 4. X-ray mapping of elements within the laterite. Elements analyzed: Ni, Si, Cr, Fe, Mg, and Al. Note the presence of the grain of chromite in upper right-hand corner which has an absence of Ni, but contains Al and Mg. Si is also distributed throughout the ooid. Goethite and hematite are distinguishable within the Fe image.

Table 5. Distribution of main elements amongst minerals of the laterite sample.

Distribution of:	Magnetite%	Chromium%	Quartz%	Fe-oxides%	Carbonates%	Others%	Total
Nickel	1.43	0.20	-	93.23	-	5.14	100
Magnesium	-	5.75	-	3.80	90.45	-	100
Aluminum	1.15	39.59	-	58.31	0.95	-	100
Silicon	0.31	0.05	89.00	10.01	0.63	-	100
Iron	8.35	2.61	-	87.47	1.56	-	100
Chromium	0.41	78.75	-	20.84	-	-	100
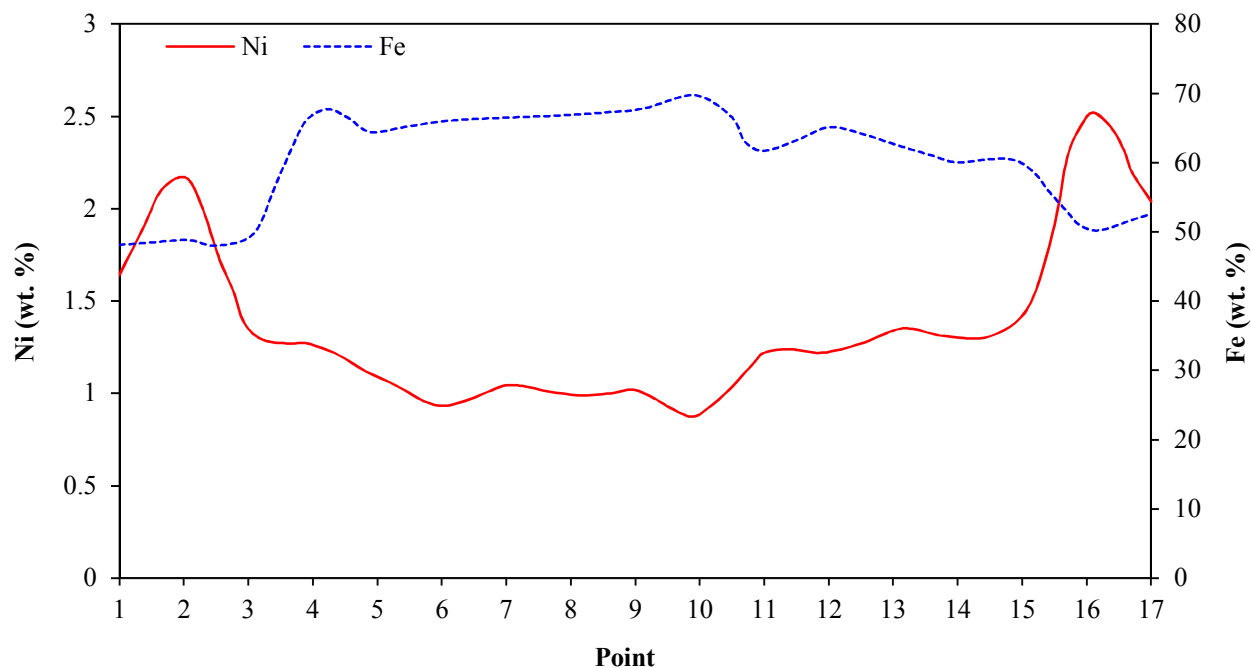
Figure 5. EDS line profile analysis of ooid consisting of hematite and goethite.
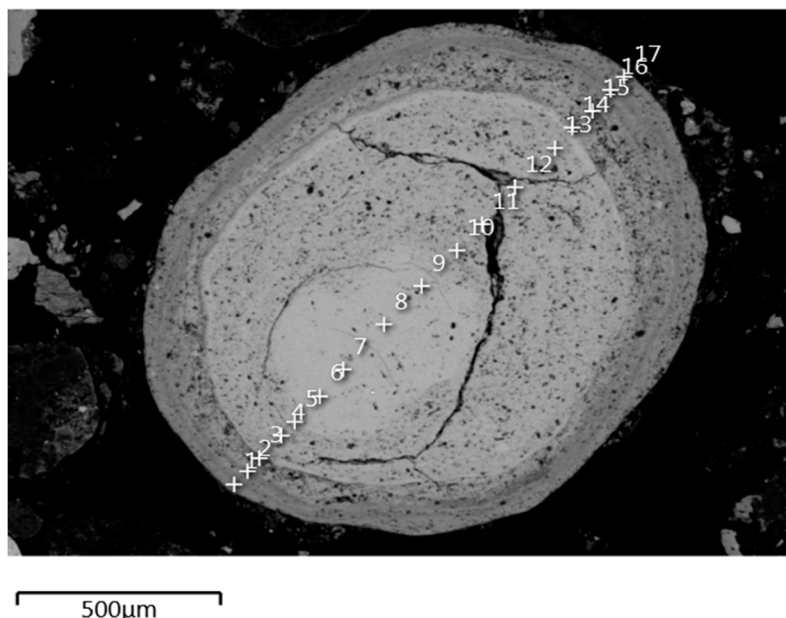
Figure 6. EDS line profile analysis of ooids consisting of hematite and goethite.

3. Conclusions

Nickel laterite sampled in order to carry out mineralogical study. Nickel content in the laterite sample was 0.7 wt. %, occurring mainly in hematite and goethite. Laterite type could be classified as limonite type of ore. Nickel distribution is confined predominantly to hematite and goethite (93.23%). A minor amount of nickel

is present within chromite and magnetite. Other minerals carry a total of 5.14% nickel and includes the relict pyroxenes and olivine that is only found in trace quantities. The distribution of main elements could be found from Table 5. Magnesium is carried mostly within dolomite and some within chromite. Iron oxides often carry a small percentage of magnesium as well. Iron is mostly distributed within hematite, magnetite, and goethite as expected. However, small amounts are present in chromite and the carbonate minerals. Approximately 300 data points were used to find any indication that nickel concentration is either elevated or depressed in the presence of other elements. Elements compared were: Al, Mg, Fe, Cr, O, and Si. The results were that nickel element concentration shows no true correlation between its appearance and any other element. EDS line profile analyses were completed on hematite/goethite ooids and there was a slight correlation in the quantities between iron and nickel in each individual ooid. However, iron and nickel do not always show a positive correlation. In some grains, there is a negative correlation between nickel and iron. Aluminum is mostly carried within goethite, hematite, and chromite and is present in minor amounts within magnetite and carbonates. Silicon is mostly found in quartz, though some is found within hematite and goethite. Chromium is mostly found within chromite, but some is also found within the hematite and goethite grains. As selectivity between gangue elements and nickel was insufficient, magnetic separation is not recommended.

Acknowledgments

References

[1]. Jang, H.C. and Valix, M. (2017). Overcoming the bacteriostatic effects of heavy metals on Acidithiobacillus thiooxidans for direct bioleaching of saprolitic Ni laterite ores. Hydrometallurgy. 168: 21-25.

[2]. Rubisov, D.H. and Papangelakis, V.G. (2000). Sulphuric acid pressure leaching of laterites—a comprehensive model of a continuous autoclave. Hydrometallurgy. 58 (2): 89-101.

[3]. Baghalha, M., Papangelakis, V.G. and Curlook, W. (2007). Factors affecting the leachability of Ni/Co/Cu slags at high temperature. Hydrometallurgy. 85 (1): 42-52.

[4]. Chalkley, M.E., Collins, M.J., Iglesias, C. and Tuffrey, N.E. (2010). Effect of magnesium on pressure leaching of Moa laterite ore. Canadian Metallurgical Quarterly. 49 (3): 227-234.

[5]. Wang, Z., Chu, M., Liu, Z., Wang, H., Zhao, W. and Gao, L. (2017). Preparing Ferro-Nickel alloy from low-grade laterite nickel ore based on metallized reduction–magnetic separation. Metals. 7 (8): 313.

[6]. Motteram, G., Ryan, M., Berezowsky, R. and Raudsepp, R. (1996). Murrin Murrin Nickel/Cobalt Project: Project Overview and Development, ALTA 1996 Nickel/Cobalt Pressure Leaching and Hydrometallurgy Forum. ALTA Metallurgical Services, Melbourne, 28.

[7]. Dhawan, N., Safarzadeh, M.S., Miller, J.D., Moats, M.S. and Rajamani, R.K. (2013). Crushed ore agglomeration and its control for heap leach operations. Minerals Engineering. 41: 53-70.

[8]. Readett, D. and Fox, J. (2011). Agglomeration–the key to success for the Murrin Murrin Ni laterite heap leach. Proceedings of MetPlant. pp. 506-514.

[9]. Nosrati, A., Addai-Mensah, J. and Skinner, W. (2012). Gelation of aqueous clay mineral dispersions leaching at low pH: Effect of mineral/pulp composition and temperature. Powder technology. 223: 98-104.

[10]. Agatzini-Leonardou, S. and Zafiratos, I.G. (2004). Beneficiation of a Greek serpentinic nickeliferous ore Part II. Sulphuric acid heap and agitation leaching. Hydrometallurgy. 74 (3-4): 267-275.

[11]. Luo, W., Feng, Q., Ou, L., Zhang, G. and Chen, Y. (2010). Kinetics of saprolitic laterite leaching by sulphuric acid at atmospheric pressure. Minerals Engineering. 23 (6): 458-462.

[12]. McDonald, R.G. and Whittington, B.I. (2008). Atmospheric acid leaching of nickel laterites review: Part I. Sulphuric acid technologies. Hydrometallurgy. 91 (1-4): 35-55.

[13]. Göveli, A. (2006). Nickel extraction from gördes laterites by hydrochloric acid leaching (Doctoral dissertation, MSc Thesis, Middle East Technical University, Ankara, Turkey).

[14]. Janwong, A. (2012). The agglomeration of nickel laterite ore (Vol. 74, No. 04).

[15]. Norgate, T. and Jahanshahi, S. (2010). Low grade ores–smelt, leach or concentrate?. Minerals Engineering. 23 (2): 65-73.

[16]. Curlook, W. (2002). U.S. Patent No. 6,379,637. Washington, DC: U.S. Patent and Trademark Office.

[17]. Canterford, J.H. (1978). Leaching of some Australian nickeliferous laterites with sulphuric acid at atmospheric pressure.

[18]. Kyle, J. (2010). Nickel laterite processing

technologies–where to next?.

[19]. Macnaughton, S.J., Ring, R.J., Day, A., Collier, D.E. and Tan, L.K.P. (1999). Optimisation of the leach conditions for a copper/uranium ore. In EPD Congress (pp. 509-522). Proceeding of Sessions and Symposia Minerals, Metals and Materials Society San Diego.

[20]. Nosrati, A., Addai-Mensah, J. and Skinner, W. (2009). pH-mediated interfacial chemistry and particle interactions in aqueous muscovite dispersions. Chemical engineering journal. 152 (2-3): 406-414.

[21]. Nosrati, A., Addai-Mensah, J. and Robinson, D.J. (2012). Drum agglomeration behavior of nickel laterite ore: Effect of process variables. Hydrometallurgy. 125: 90-99.

[22]. Tan, H., Skinner, W. and Addai-Mensah, J. (2012). Leaching behaviour of low and high Fe-substituted chlorite clay minerals at low pH. Hydrometallurgy. 125: 100-108.

[23]. López-Galindo, A., Viseras, C. and Cerezo, P. (2007). Compositional, technical and safety specifications of clays to be used as pharmaceutical and cosmetic products. Applied Clay Science. 36 (1-3): 51-63.

[24]. Bodas, M.G. (1996). Hydrometallurgical treatment of zinc silicate ore from Thailand. Hydrometallurgy. 40 (1-2): 37-49.

[25]. Griffin, A., Nofal, P., Johnson, G. and Evans, H. (2002). Laterites- squeeze or ease. In Pressure Leaching and Hydrometallurgy Forum, ALTA. pp. 2-16.

[26]. Elias, M. (2002). Nickel laterite deposits-geological overview, resources and exploitation. Giant ore deposits: Characteristics, genesis and exploration. CODES Special Publication. 4: 205-220.

[27]. McDonald, R.G. and Whittington, B.I. (2008). Atmospheric acid leaching of nickel laterites review. Part II. Chloride and bio-technologies. Hydrometallurgy. 91 (1-4): 56-69.

[28]. Guo, Z., Zhu, D., Pan, J. and Zhang, F. (2017). Mineralogical Characteristics and Preliminary Beneficiation of Nickel Slag from Reduction Roasting-Ammonia Leaching. Minerals. 7 (6): 98.

[29]. Das, G.K. and De Lange, J.A.B. (2011). Reductive atmospheric acid leaching of West Australian smectitic nickel laterite in the presence of sulphur dioxide and copper (II). Hydrometallurgy. 105 (3-4): 264-269.

[30]. Briceno, A. and Osseo-Asare, K. (1995). Particulates in hydrometallurgy: Part II. Dewatering behavior of unflocculated laterite acid leach residues.

Metallurgical and Materials Transactions B. 26 (1): 1133-1138.

[31]. Dijkstra, M., Hansen, J.P. and Madden, P.A. (1995). Gelation of a clay colloid suspension. Physical review letters. 75 (11): 2236.

[32]. Büyükakinci, E. and Topkaya, Y.A. (2009). Extraction of nickel from lateritic ores at atmospheric pressure with agitation leaching. Hydrometallurgy. 97 (1-2): 33-38.

[33]. Senanayake, G., Childs, J., Akerstrom, B.D. and Pugaev, D. (2011). Reductive acid leaching of laterite and metal oxides- a review with new data for Fe (Ni, Co) OOH and a limonitic ore. Hydrometallurgy. 110 (1-4): 13-32.

[34]. Cabri, L.J., Wilhelmij, H.R. and Eksteen, J.J. (2017). Contrasting mineralogical and processing potential of two mineralization types in the platinum group element and Ni-bearing Kapalagulu Intrusion, western Tanzania. Ore Geology Reviews. 90: 772-789.

[35]. Crundwell, F., Moats, M., Ramachandran, V., Robinson, T. and Davenport, W.G. (2011). Extractive metallurgy of nickel, cobalt and platinum group metals. Elsevier.

[36]. Dalvi, A.D., Bacon, W.G. and Osborne, R.C. (2004). The past and the future of nickel laterites. In PDAC 2004 International Convention, Trade Show & Investors Exchange (pp. 1-27). Toronto: The prospectors and Developers Association of Canada.

[37]. Lamya, R.M. (2007). A fundamental evaluation of the atmospheric pre-leaching section of the nickel-copper matte treatment process (Doctoral dissertation, Stellenbosch: University of Stellenbosch).

[38]. Liu, K., Chen, Q., Hu, H., Yin, Z. and Wu, B. (2010). Pressure acid leaching of a Chinese laterite ore containing mainly maghemite and magnetite. Hydrometallurgy. 104 (1): 32-38.

[39]. Mohammed, W.T., Ahmedzeki, N.S. and AbdulNabi, M.F. (2011). Extraction of valuable metals from spent hydrodesulfurization catalyst by two stage leaching method. Iraqi Journal of Chemical and Petroleum Engineering. 12 (4): 21-35.

[40]. Swamy, K.M., Sukla, L.B., Narayana, K.L., Kar, R.N. and Panchanadikar, V.V. (1995). Use of ultrasound in microbial leaching of nickel from laterites. Ultrasonics Sonochemistry. 2 (1): S5-S9.

[41]. Tang, J. and Valix, M. (2004). Leaching of low-grade nickel ores by fungi metabolic acids.

[42]. Van Lier, R.J. (1996). Analysis of the first-stage leach process at Inco Ltd.'s copper refinery (Doctoral dissertation, University of British Columbia).

نگاشت اشعه X و الگوی کانی‌شناسی کانی لاتریت نیکل‌دار در بوانات فارس ایران

احمد عباسی قرائی'، بهرام رضایی'² و هادی حمیدیان شورمستی³

۱ -گروه مهندسی معدن دانشگاه آزاد اسلامی واحد علوم و تحقیقات، تهران، ایران

۲- دانشکده مهندسی معدن و متالورژی، دانشگاه صنعتی امیرکبیر، ایران

۳- گروه مهندسی معدن دانشگاه آزاد اسلامی واحد قائم‌شهر، ایران

چکیده:

با توجه به طبقه‌بندی لاتریت‌های نیکل‌دار، این پژوهش، تست‌های کانی‌شناسی که عناصر ارزشمند که در آن به فرم کانه معدنی می‌باشد را توضیح می‌دهد. بر اساس ترکیب شیمیایی این لاتریت نیکل‌دار به عنوان یک نوع لیمونیت طبقه‌بندی شده و محتوای نیکل و کبالت آن به ترتیب ۰/۷ و ۰/۰۴ درصد می‌باشد کـه عمدتاً نیکل با هماتیت و گوتیت همراه است. بر اساس تجزیه کانی‌شناسی سنگ معدن مشاهده می‌شود که بخش قابل‌تـوجهی از نیکـل در هماتیـت قـرار دارد. بنابراین نیکل را نمی‌توان از شبکه هماتیت جدا کرد. مقدار نیکل در لاتریت ۰/۷ درصد و مقدار کبالت ۰/۰۴ درصد می‌باشد و ترکیب شیمیایی لاتریـت برابـر بـا ۳۸/۹ درصد اکسیدهای آهن، ۲۶/۹ درصد کربنات‌ها، ۲۶/۹ درصد کوارتز، ۴/۸ درصد کرومیت، ۲/۷ درصد مگنتیت و سایر مـواد معـدنی ۱/۹ درصـد مـی‌باشـد. تجزیه‌وتحلیل پروفایل‌های EDS بر روی اوئیدها در هماتیت و گوتیت نشان می‌دهد همبستگی کمی بین آهن و نیکل در هر اوئید وجود دارد، با این حال آهن و نیکل همیشه یک ارتباط مثبت نشان نمی‌دهد و تنها عیار نیکل در جداسازی مغناطیسی از ۰/۷ درصد به ۰/۹ درصد افزایش میابد. اگرچه بازیابی نیکل ۴۵ درصد می‌باشد.

کلمات کلیدی: لاتریت‌ها، نیکل، کانی‌شناسی، آنالیز پروفایل خطوط EDS.